XII International Conference on Computational Plasticity. Fundamentals and Applications
COMPLAS XII
E. Oñate, D.R.J. Owen, D. Peric and B. Suárez (Eds)

CRACK PROPAGATION IN THIN SHELLS BY EXPLICIT DYNAMICS SOLID-SHELL MODELS

Mara Pagani, Umberto Perego*

Department of Civil and Environmental Engineering
Politecnico di Milano
Piazza L. Da Vinci 32, 20133 Milano, Italy
e-mail: pagani@mail.polimi.it, umberto.perego@polimi.it

Key words: Explicit dynamics, solid shell elements, cohesive fracture, cutting.

Abstract. A computational technique for the simulation of crack propagation due to cutting in thin structures is proposed. The implementation of elastoplastic solid-shell elements in an explicit framework is discussed. Finally, in the case of crack propagation, the issue of the selection of a propagation criterion is briefly discussed. Crack propagation is modelled making use of a so called "directional" cohesive approach.

1 INTRODUCTION

The numerical simulation of cutting of thin structures is of interest in many engineering fields since it occurs in many applications, such as metal forming, bioengineering, naval and aerospace engineering. The simulation of this kind of problems has to cope with several types of nonlinearities such as contact, large strain, plasticity and fracture. Moreover, the computational treatment of thin structures requires the use of special kind of finite elements. In the present contribution a computational strategy is presented based on the implementation of a reduced integration solid-shell element in an explicit framework, in conjunction with a cohesive approach to fracture. Solid-shell elements are preferred since, among other features, they allow for a straightforward incorporation of complex 3D material models, are easy to use in combination with 3D solid elements, and they offer good accuracy in the through-the thickness stress distribution.

Solid-shell elements have been predominantly used in the framework of implicit formulations and exhibit some features which may lead to an increase of computational costs when implemented in an explicit dynamics code. Solid-shell elements are known to suffer locking problems, such as shear locking, which is typically cured by ANS (Assumed Natural Strain) method, and volumetric locking, which is usually controlled by means of EAS (Enhanced Assumed Strain) method. The latter method, requiring the implicit solution of a nonlinear problem for the computation of the enhanced variables, is particularly ex-

pensive in terms of computational effort. To reduce computational costs, explicit update of the enhanced variables has been proposed.

An additional problem is represented by the fact that solid-shell elements have a dimension, the thickness, which is significantly smaller that the other two dimensions. This leads to a high finite element maximum eigenfrequency and, consequently, to a very small stable time step. In the present work the selective mass scaling technique, based on a linear transformation of the degrees of freedom, proposed in [1] is applied to increase the stable time step without affecting the dynamical response. Moreover, an analytical procedure is introduced for the computation of the highest eigenfrequency and estimate of the critical time-step size of the scaled system, together with a strategy for the optimal choice of the scaling factor which is described in section 2.

The simulation of cutting requires the development of ad hoc strategies different from standard approaches to fracture. Classical interface cohesive elements, where the cohesive forces are transmitted in the direction of the crack opening displacement, cannot correctly reproduce situations where the blade interferes with the active process zone. A simplified approach, based on the new concept of "directional cohesive elements" (see [2]), is proposed and described in section 3. The proposed approach is applicable to thin sheets, since it does not account for through the thickness crack propagation.

These features have been implemented into an explicit finite element code, in addition to standard features, such as large strain plasticity and contact which are necessary for the simulation of cutting problems. Section 4 summarizes the operative strategy while in section 5 comparisons with analytical and experimental results are presented to show the potentiality of the method and to single out possible defects and limitations.

2 SOLID SHELL ELEMENTS AND EXPLICIT DYNAMICS

In order to describe the behavior of thin structures the 8-node solid-shell element recently proposed by Schwarze and Reese (see [3]) has been used for the development of the computational model. The element is based on a reduced integration with hourglass control and implements ANS (Assumed Natural Strain) and EAS (Enhanced Assumed Strain) technologies to avoid the various type of locking behavior that affect this type of low order solid-shell elements. The computation of the enhanced strain parameter and the critical time step size can become computationally critical in explicit dynamics and the strategy adopted to circumvent the problem is briefly described below.

2.1 Enhanced Assumed Strain (EAS) method

The Q1STs element adopts the enhanced assumed strain method to cure volumetric and Poisson locking. Considerations about the strain modeling lead to the introduction of only one enhanced degree of freedom. However, since the computation of the enhanced term requires the solution of a nonlinear equation at each time step, it becomes critical in terms of computing time when the time step size is very small, as it happens in most

cases in explicit dynamics simulations. As a possible remedy, consistent with the explicit character of the adopted time integration scheme, the computation at each time step of an explicit estimate of the increment ΔW_e of the enhanced variable W_e is proposed. The obtained explicit estimate of $W_e = W_e + \Delta W_e$ is to be used in the next step for the constitutive update. Numerical tests have shown that the explicit estimate preserves the accuracy of the implicit one, while it can provide savings of the order of 50% in computing time.

2.2 Selective mass scaling

The main disadvantage of using solid-shell elements in combination with explicit time integration scheme is the small critical time step determined by the thickness of the structure. To overcome this problem in [1] a selective mass scaling technique has been proposed which influences only the higher order structural eigenmodes affecting the critical time step. The idea is then based on a linear transformation of the solid-shell element degrees of freedom, which allows to selectively apply the mass scaling while preserving the mass lumping.

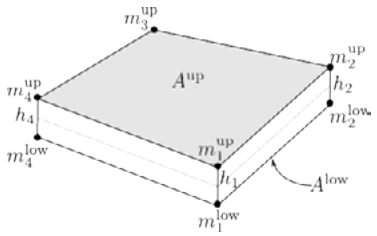

Figure 1: Solid-shell element: definition of upper and lower surfaces.

Once upper and lower surfaces of the eight-node solid-shell element are identified (Figure 1), we denote with $\mathbf{a}_i^{up}$ and $\mathbf{a}_i^{low}$, $i = 1, \ldots, 4$ the accelerations of corresponding nodes on the two surfaces. The accelerations $\mathbf{a}_i^{ave}$, governing the element rigid body modes, can be defined using the following linear transformation

$$\mathbf{a}_i^{ave} = \frac{\mathbf{a}_i^{up} + \mathbf{a}_i^{low}}{2} \tag{1}$$

while the accelerations $\mathbf{a}_i^{diff}$, governing the higher order modes, are defined as

$$\mathbf{a}_i^{diff} = \frac{\mathbf{a}_i^{up} - \mathbf{a}_i^{low}}{2}. \tag{2}$$

In matrix form we have

$$\underset{24\times1}{\mathbf{a}^e} = \left\{ \begin{array}{c} \underset{12\times1}{\mathbf{a}^{up}} \\ \underset{12\times1}{\mathbf{a}^{low}} \end{array} \right\}^e = \mathbf{T}\hat{\mathbf{a}}^e = \left[\begin{array}{cc} \mathbf{I} & \mathbf{I} \\ \mathbf{I} & -\mathbf{I} \end{array} \right]^e \left\{ \begin{array}{c} \underset{12\times1}{\mathbf{a}^{ave}} \\ \underset{12\times1}{\mathbf{a}^{diff}} \end{array} \right\}^e, \quad \hat{\mathbf{M}}^e = \mathbf{T}^T\mathbf{M}^e\mathbf{T} \tag{3}$$

where a superposed hat denotes vectors and matrices expressed in terms of average and difference degrees of freedom. The idea is to change the component of the mass matrix $\hat{\mathbf{M}}^e$ correlated with the higher modes contained in $\mathbf{a}_e^{diff}$:

$$\hat{\mathbf{M}}^e_{lumped} = \begin{bmatrix} \underset{12\times12}{\mathbf{M}^{ave}} & \mathbf{0} \\ \mathbf{0} & \alpha \underset{12\times12}{\mathbf{M}^{diff}} \end{bmatrix}^e . \tag{4}$$

After the mass scaling is carried out, the analytical estimate of the maximum eigenfrequency of the scaled element, corresponding to the thickness vibration mode, proposed by [1] can be used to determine the critical time step size. The scaling parameter α has to be optimized so as to maximize the time-step size without significant accuracy losses. Since for high values of α the critical time step Δt exhibits an asymptote revealing that the critical time-step size becomes determined by the in-plane traversal time, values of α above this limit would be completely useless. The optimal value of α to be used for mass scaling is assumed to be the one which guarantees a stable time-step size corresponding to the 90% of the asymptotic value.

3 CRACK PROPAGATION

Using the finite element method to perform cutting simulations, one of two possible approaches is usually adopted: the element deletion method and the node separation method. Other approaches, based on the enrichment of the element kinematics to incorporate the displacement discontinuity are less frequently used in explicit dynamics. In the element deletion method, when the fracture criterion is satisfied at an element, the stiffness of the element is set to zero. From a physical point of view, it is difficult to justify the element deletion and the result is strongly affected by the element size with respect to other geometric characteristics. On the other hand, in the node separation method, when the fracture criterion is satisfied at a node, the node itself is duplicated and the connectivity of neighboring elements has to be changed. Even if this method is more difficult to implement, the physical meaning is clear. The drawback is that the crack can propagate only along directions coinciding with element edges, which are pre-determined by the mesh layout. The problem can be alleviated using a local adaptive remeshing or a very fine mesh since the beginning. One argument in favour of the node separation method in cutting problems is that the main crack propagation direction is dictated by the imposed blade movement so that the mesh can be a priori adjusted to follow the correct propagation path, thus reducing the topological approximation intrinsic in this type of approaches, without the need to use extremely refined meshes. Our strategy models fracture propagation by means of the node separation method in combination with the "directional" cohesive element proposed in [2] and the definition of an ad hoc fracture criterion.

3.1 Directional cohesive elements

In classical cohesive elements cohesive forces are typically transmitted in the direction of the crack opening displacement, an approximation which can give rise to inaccurate predictions of the crack propagation when the fracture of a very ductile material is the consequence of the impact with a sharp object. When the material is quasi-brittle and/or the impacting object is blunt, there is no interference between the object and the cohesive region because the ultimate cohesive opening displacement is much smaller than the typical size of the object. On the contrary, when the material is very ductile or the cutting blade is sharp, it may happen that the blade intersects the trajectory of the cohesive forces. To account for these possible interactions, a new type of cohesive interface element to be interposed between adjacent separating solid-shell elements, the so-called "directional" cohesive element, is applied in this context. The operative sequence is very simple. When a suitable fracture criterion is met at a given node, the node is duplicated and it is assumed that cohesive forces $\mathbf{f}_a^{\pm}$ are transmitted between the newly created pair of nodes $a^{\pm}$ by a massless string, i.e. a truss element introduced ad hoc in the model in correspondence of each pair of separating nodes (Figure 2). During subsequent time steps, the nodes separate and the string, which initially is a straight segment naturally endowed with a length ℓ which is simply the distance between the nodes, elongates. The direction of the cohesive force is determined by the opening vector while the intensity of the force depends on the specific cohesive constitutive law adopted for the string.

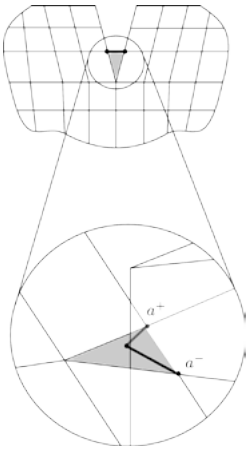

Figure 2: Detail of genesis of a string element and its interaction with the blade.

The cable element is a well defined geometric entity, and its contact against the cutting blade can be checked throughout the analysis duration. When a point of a cable element is detected to be in contact with the blade, the cable element is subdivided in two truss elements by introducing a joint in correspondence to the contact point. The length of the cable is now defined as the sum of the lengths of the two constituent truss elements.

It is here assumed that the contact point cannot move along the cutting edge of the cutter. Two forces $\mathbf{f}_a^+$ and $\mathbf{f}_a^-$ of the same magnitude are assumed to be transmitted by the two branches of the cable to the crack flanks. The direction of the forces is however different at the two nodes a^+ and a^-, being determined by the directions of the truss elements connecting the nodes to the contact point (see Figure 2). The force magnitude in the cable is obtained from the adopted cohesive law and is a function of the total cable length ℓ. In this way, the cohesive force can be transmitted between the crack flanks in a direction which is not along the line connecting the separating nodes, correctly taking into account the presence of the cutter.

3.2 Fracture criterion

One of the main issues in the simulation of fracture processes is the definition and calibration of a fracture criterion. In the case of elastic fracture, the most widespread criterion is based on the evaluation of principal stresses. On the other hand, since in ductile fracture failure is the combined result of nucleation, growth and coalescence of microscopic defects, the prediction of the fracture inception is prone to different interpretations giving rise to a large number of fracture criteria.

In view of its simplicity and acceptable accuracy, for our simulations we have chosen to implement the widely used equivalent plastic strain criterion

$$\int_0^{\varepsilon_f^p} H(\sigma_H)\ \mathrm{d}\varepsilon^p = \varepsilon_{\mathrm{cr}}^p \tag{5}$$

which simply uses ε^p as the driving quantity for fracture initiation. The term $H(\sigma_H)$, σ_H being the hydrostatic stress component and H being the Heaviside function, has been here introduced to guarantee that fracture occurs only under tensile stress conditions. Detailed validation tests have shown that, despite its simplicity, this criterion provides excellent results in the simulation of crack propagation in metal plates. Once the critical plastic strain is attained at a node, the crack is allowed to propagate along the direction dictated by the maximum principal Cauchy stress at the same node.

4 OPERATIVE STRATEGY

The proposed strategy has been programmed in a Fortran 90 parallel code for shared memory architectures using an explicit central finite difference time integration scheme together with the described selective mass scaling. Once the structure is discretized by means of solid-shell finite elements, the optimal value of the scaling parameter α which guarantees the maximization of the time step size, is computed. As the critical time step is estimated, the operative sequence summarized in Figure 3 is followed to solve the cutting problem. The computation of internal forces and the fracture algorithm are the most complex and computationally expensive operations of the procedure.

The computation of the equivalent nodal internal force vector requires the evaluation

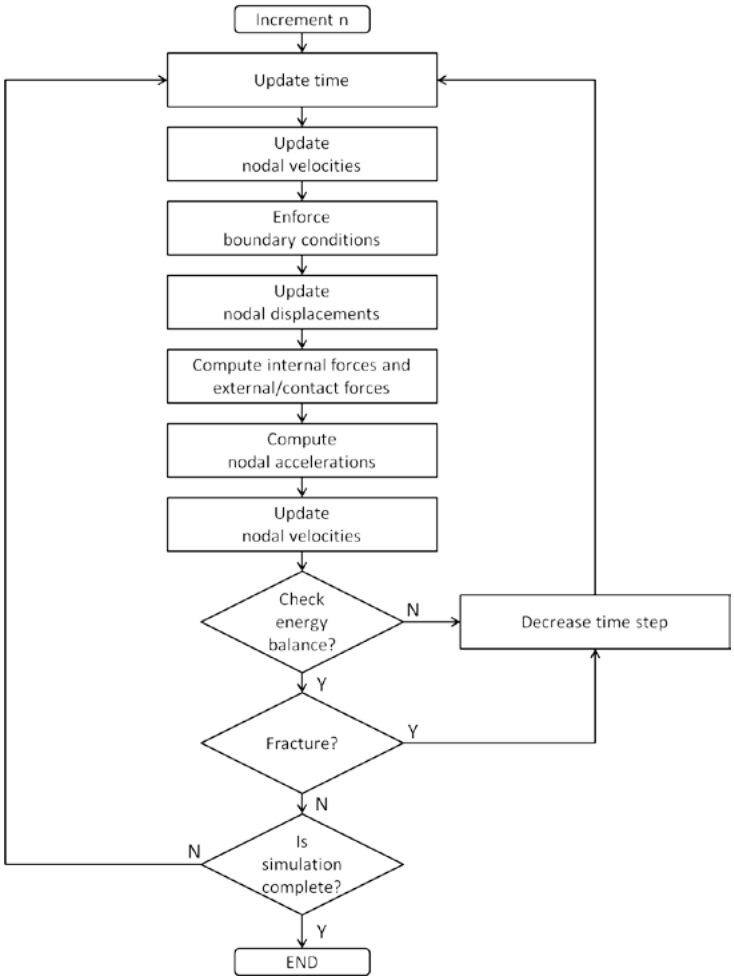

Figure 3: Flowchart.

of the compatible Green Lagrange strain vector and the explicit update of the enhanced strain variable W_e to be used in the next time step.

The fracture initiation and propagation procedure is managed at nodal level. To check if a fracture propagates we need the nodal values of the equivalent plastic strain and of the Cauchy stress tensor, which are required for the application of the fracture initiation criterion, for the determination of the fracture propagation direction and for the definition of the initial value of the nodal cohesive force. Since all the information about these quantities is stored at Gauss points along the thickness of the element, a strategy which extrapolates the nodal values of stresses and strains has to be defined. It is also important to be able to distinguish between uncracked nodes (i.e. nodes where only uncracked element sides are converging) and tip nodes (i.e. nodes at the uncracked tip of a cracked element side). In fact, experimental results show that uncracked nodes may require a

higher plastic deformation threshold than tip nodes to propagate a fracture. This distinction defines also different strategies for the extrapolation of nodal values of stresses and strains.

- In case of uncracked nodes, the patch composed of all elements sharing the node under consideration is built. Stress and strain values at $\mathbf{x}_a^{\text{mid}}$, which is the position of the intersection between the middle surface and the line connecting corresponding upper and lower nodes are extracted. Denoting by index i the Gauss points at the $i-$th thickness level, the procedure, composed of two steps, can be described as follows:

  1. For Gauss points at level i, an average nodal value of Cauchy stress $\boldsymbol{\sigma}_i^{\text{ave}}$ and of equivalent plastic strain $\varepsilon_i^{p\,\text{ave}}$ is computed among all the elements in the patch.
  2. New middle plane values $\boldsymbol{\sigma}^{\text{mid}}$ and $\varepsilon^{p\,\text{mid}}$ are obtained starting from the previously defined $\boldsymbol{\sigma}_i^{\text{ave}}$ and $\varepsilon_i^{p\,\text{ave}}$ by computing the average among nodal values at the different levels.

- The same procedure used for the extrapolation of nodal information described for the uncracked nodes is also used for the tip nodes, except for the construction of the element patch. In this particular case, only values from the elements located ahead of the tip in the direction of the fracture propagation are used.

The nodal Cauchy stress and equivalent plastic deformation values are used to check if the fracture nucleates or not according to the criterion (5). When the fracture criterion is exceeded at a given node a, the node is duplicated and the crack is assumed to propagate along the element edge whose normal is closer to the maximum principal stress direction.

5 NUMERICAL EXAMPLES

Some numerical examples are presented in order to validate the proposed method for the simulation of cutting of thin-walled structures.

5.1 Notched cylinder fracture under internal detonation pressure

The first example of application of the proposed strategy deals with the dynamic fracture of a notched cylinder. In [4], a series of experiments were conducted to observe the fracture behavior of thin-walled and initially flawed aluminum tubes under internal gaseous detonation loading. Since one of the objectives was the study of the qualitative pattern of the crack path of a fractured tube as a function of initial flaw length, a series of experiments on aluminum 6061-T6 tubes, keeping constant the notch depth (0.56 mm), the notch width (0.3 mm), the tube size (0.88 mm thick, 38 mm in diameter and 914 mm long as in Figure 4) and loading conditions, but changing the notch length were conducted. Different fracture behavior was observed for the various notch lengths. As the notch length increased, the crack propagated further and severed the tube into two or

three parts. We have chosen to simulate the experiment with initial notch $L = 12.7$ mm.

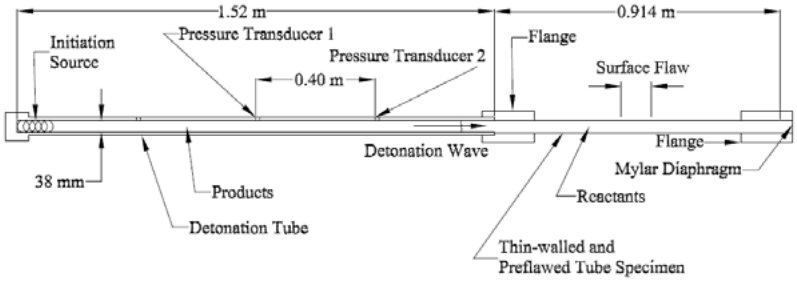

Figure 4: Notched cylinder fracture under internal detonation pressure. Tube assembly with 914 mm long specimen [4].

Even if our procedure has been developed for the simulation of cutting problem, we are also interested in the validation of the overall strategy in situations where the crack path is not dictated by any blade. Other approaches could be more effective for this type of problem than the "directional" cohesive elements here considered. In particular, the propagation direction is expected to be affected by the mesh layout.

The cylinder has been discretized by 26448 solid-shell elements and the resulting optimal scaling parameter $\alpha_{\text{opt}} = 6.3$ leads to a stable time step of $\Delta t = 2.7 \cdot 10^{-7}$ s. The shell material has been modeled with J_2-plasticity, density $\rho = 2.78 \cdot 10^{-9}$ Ns^2/mm^4, Young's modulus $E = 69000$ MPa, Poisson's ratio $\nu = 0.3$, yield stress $\sigma_y = 275$ MPa and by means of a linear isotropic hardening with constant slope $H = 640$ MPa. A cohesive fracture energy $G_f = 12$ kJ/m^2 has been considered on the basis of the stress intensity factor $K_{cr} = 30$ MPa$\sqrt{\text{m}}$, reported in [4]. As in [5], who also analyzed one of the tests carried out by Chao and Shepherd, fracture propagation starting from tip nodes has been favored in order to avoid fragmentation.

The detonation wave has been modeled by means of a suitable time history function.

Figure 5 shows a comparison of the final deformed shape between the simulation and the experimental results. Both pictures have been reproduced at the same scale in order to provide a clear visual comparison. Despite some discrepancies as expected, in the crack path, the simulation is in good qualitative agreement with the experiment, also in terms of crack propagation path length.

5.2 Cutting of a rubber plate by a wedge

In [6] Lake and Yeoh conducted a series of experiments for assessing the resistance of pre-stretched rubber sheets to cutting by sharp objects under conditions where friction is minimized. The special behavior of rubber requires the adoption of razor blades as

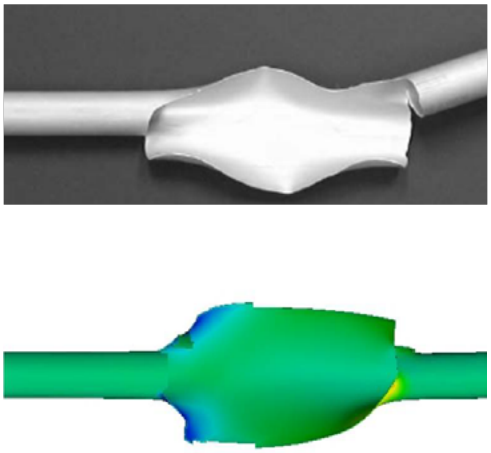

Figure 5: Notched cylinder fracture under internal detonation pressure. Comparison of final deformed shapes. Above: the experimental result. Below: simulation results.

cutting implements to avoid the specimen buckling. These experiments have highlighted the importance of the pre-stretching of the rubber sheets to guarantee the cutting of the specimen. In particular, the existence of a minimum value of pre-stretching elastic strain energy below which no fracture propagates has been pointed out. On the other hand, a threshold value of elastic strain energy which gives rise to unstable propagation of fracture has also been estimated. These features become evident if the rubber sheet is cut by a razor. Unfortunately, even using our "directional" cohesive elements, the numerical simulation of the local stress intensification preceding crack initiation, due to a razor blade, would require the use of a very refined mesh with element dimensions which have to compare with the curvature radius of the cutter.

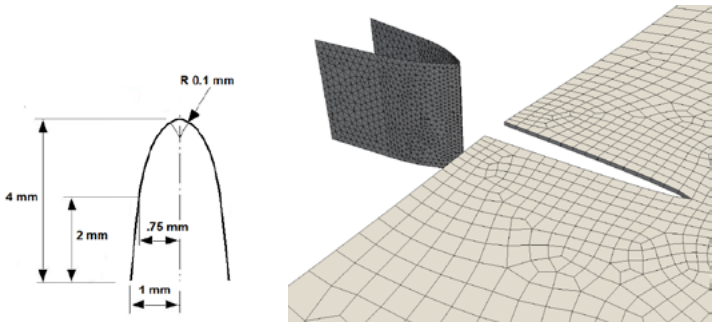

Figure 6: Cutting of a rubber plate. Blade geometry.

In our investigation we have therefore adopted a wedge blade with a curvature radius 0.1 mm (Figure 6) to simulate the cutting of a pre-stretched rubber sheet 32 mm wide, 40 mm long, 0.1 mm thick, with a crack of 5 mm parallel to its long edges. Since the

mechanical properties of the used rubber sheets were not specify in [6], we have considered a low quality rubber modeled by a Neo Hookean hyperelastic material, with properties taken from the literature: shear strength 1 MPa, Poisson's coefficient $\nu = 0.49$, material density $\rho = 1 \cdot 10^{-9}$ Ns^2/mm^4. A reference tear strength of about 2.0 N/mm^2 has been used associated to a fracture energy $G_f = 3$ N/mm.

The sheet has been discretized by means of 6514 solid-shell elements, mainly concentrated along the expected fracture path around the symmetry axis. A stable time step $\Delta t = 4.10 \cdot 10^{-6}$ s is guaranteed by a small optimal scaling parameter $\alpha_{\text{opt}} = 3.5$. In order to further reduce the computational time, the density of all elements has been uniformly increased by a factor 100. The wedge has been assigned a velocity of 96 mm/s, which is much faster than the real blade velocity reported in the experiments (of the order of mm/hr). We have conducted two distinct simulations keeping constant the fracture energy and the initial pre-stretching of 5.76 mm (corresponding to a uniform nominal strain of 18%) and varying the tear strength of about 20%. As expected, we have obtained a completely different behavior of the specimen in the two cases. In the first case, with a tear strength $T_0 = 2.0$ N/mm^2 a stable cutting has been obtained. After the initial pre-stretching, only the first two nodes were already cracked and a stable crack started to develop as soon as the blade got in contact with the plate. The interaction between the blade and the cohesive strings can be appreciated in Figure 7, which refers to the end of the analysis, corresponding to a propagation of about 20 mm.

Considering a tear strength $T_0 = 2.4$ N/mm^2, a completely different response has been obtained. The initial plate configuration after the pre-stretching phase was almost the same as in the previous case, even if now there were no cracked nodes. After contact, the blade did not succeed in promoting crack propagation. The blade contact produced a compression state ahead of the tip with the extensive buckling visible in Figure 8.

Even though a quantitative comparison with the experimental results has not been possible for the reasons specified above, the simulation has confirmed the existence of different cutting regimes depending on the relative magnitude of the tear resistance and the initial pre-stretching.

6 CONCLUSIONS

A numerical tool for the cutting simulation of thin-walled structures has been developed. Ad hoc algorithms for the simulation of fracture nucleation and propagation in the presence of an interaction with the cutting blade have been developed. A solid-shell element has been employed in an explicit framework in conjunction with a specifically devised cohesive approach to fracture. The application of the approach to the simulation of two experimental tests has provided encouraging results.

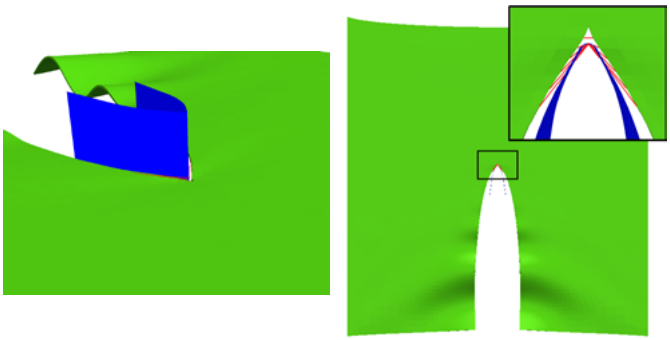

Figure 7: Cutting of a rubber plate. Final snapshots of the stable cutting process for tear strength $T_0 = 2.0$ N/mm^2.

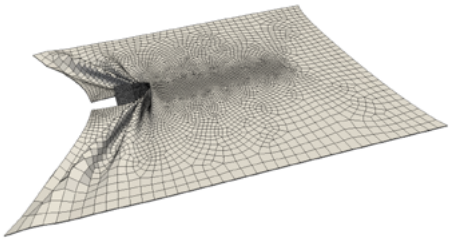

Figure 8: Cutting of a rubber plate. Buckled configuration for tear strength $T_0 = 2.4$ N/mm^2.

REFERENCES

[1] Cocchetti, G., Pagani, M. and Perego, U. Selective mass scaling and critical time-step estimate for explicit dynamics analyses with solid-shell elements. *Computers & Structures* (2012) **doi**:/10.1016/j.compstruc.2012.10.021.

[2] Frangi, A., Pagani, M., Perego, U. and Borsari R. Directional Cohesive Elements for the Simulation of Blade Cutting of Thin Shells. *CMES* (2010) **57**: 205–224.

[3] Schwarze, M. and Reese, S. A Reduced Integration Solid-Shell Finite Element Based on the EAS and the ANS Concept: Large Deformation Problems. *Int. J. Num. Meth. Engng.* (2011) **85**: 289–329.

[4] Chao, T. and Shepherd, J.. Fracture response of externally flawed aluminum cylindrical shells under internal gaseous detonation loading. *International Journal of Fracture* (2005) **134**:59–90.

[5] Song, J.-H. and Belytschko, T. Dynamic Fracture of Shells Subjected to Impulsive Loads. *Journal of Applied Mechanics* (2009) **76**:051301.

[6] Lake, G. and Yeoh, O. Measurement of rubber cutting resistance on the absence of friction. *International Journal of Fracture* (1978) **14**:509-526.